A Novel Nanobody Targeting Middle East Respiratory Syndrome Coronavirus (MERS-CoV) Receptor-Binding Domain Has Potent Cross-Neutralizing Activity and Protective Efficacy against MERS-CoV

Short title: Anti-MERS-CoV nanobody with protective efficacy

Guangyu Zhao[a], Lei He[a], Shihui Sun[a], Hongjie Qiu[a], Wanbo Tai[a,b], Jiawei Chen[b], Jiangfan Li[a], Yuehong Chen[a], Yan Guo[a], Yufei Wang[b], Jian Shang[c], Kaiyuan Ji[d], Ruiwen Fan[d], Enqi Du[e], Shibo Jiang[b], Fang Li[c#], Lanying Du[b#], Yusen Zhou[a.f#]

[a]State Key Laboratory of Pathogen and Biosecurity, Beijing Institute of Microbiology and Epidemiology, Beijing 100071, China

[b]Lindsley F. Kimball Research Institute, New York Blood Center, New York, NY 10065, USA

[c]Department of Veterinary and Biomedical Sciences, College of Veterinary Medicine, University of Minnesota, Saint Paul, MN 55108, USA

[d]ShanXi Agricultural University, Shanxi 030800, China

[e]Northwest A&F University, Shaanxi 712100, China

[f]Institute of Medical and Pharmaceutical Sciences, Zhengzhou University, Zhengzhou 450052, China

[#]Address correspondence to yszhou@bmi.ac.cn (Y.Z.) or ldu@nybc.org (L.D.).

F.L., L.D., and Y.Z. are co-senior authors of the paper and contributed equally to this work.

G.Z., L.H., and S.S. contributed equally to this work.

Abstract

The newly emerged Middle East respiratory syndrome coronavirus (MERS-CoV) continues to infect humans and camels, calling for efficient, cost-effective, and broad-spectrum strategies to control its spread. Nanobodies (Nbs) are single-domain antibodies derived from camelids and sharks, and are potentially cost-effective antivirals with small size and great expression yield. In this study, we developed a novel neutralizing Nb (NbMS10) and its human-Fc-fused version (NbMS10-Fc), both of which target the MERS-CoV spike protein receptor-binding domain (RBD). We further tested their receptor-binding affinity, recognizing epitopes, cross-neutralizing activity, half-life, and efficacy against MERS-CoV infection. Both Nbs can be expressed in yeasts with high yield, bind to MERS-CoV RBD with high affinity, and block the binding of MERS-CoV RBD to the MERS-CoV receptor. The binding site of the Nbs on the RBD was mapped to be around residue Asp539, which is part of a conserved conformational epitope at the receptor-binding interface. NbMS10 and NbMS10-Fc maintained strong cross-neutralizing activity against divergent MERS-CoV strains isolated from humans and camels. Particularly, NbMS10-Fc had significantly extended half-life *in vivo*; a single-dose treatment of NbMS10-Fc exhibited high prophylactic and therapeutic efficacy by completely protecting humanized mice from lethal MERS-CoV challenge. Overall, this study proves the feasibility of producing cost-effective, potent, and broad-spectrum Nbs against MERS-CoV, and has produced Nbs with great potentials as anti-MERS-CoV therapeutics.

Importance

Therapeutic development is critical for preventing and treating continual MERS-CoV infections in humans and camels. Because of their small size, nanobodies (Nbs) have advantages as antiviral

therapeutics (e.g., high expression yield and robustness for storage and transportation), and also potential limitations (e.g., low antigen-binding affinity and fast renal clearance). Here we have developed novel Nbs that specifically target the receptor-binding domain (RBD) of MERS-CoV spike protein. They bind to a conserved site on MERS-CoV RBD with high affinity, blocking RBD's binding to MERS-CoV receptor. Through engineering a C-terminal human Fc tag, the *in vivo* half-life of the Nbs is significantly extended. Moreover, the Nbs can potently cross-neutralize the infections of diverse MERS-CoV strains isolated from humans and camels. The Fc-tagged Nb also completely protects humanized mice from lethal MERS-CoV challenge. Taken together, our study has discovered novel Nbs that hold promise as potent, cost-effective, and broad-spectrum anti-MERS-CoV therapeutic agents.

Keywords: MERS-CoV, spike protein, receptor-binding domain, nanobody, cross-neutralization, protective efficacy

Introduction

Nanobodies (Nbs), also called camelid heavy-chain variable domains (VHHs), are single-domain nano-sized antibodies; they are derived from variable fragments of camelid or shark heavy chain-only antibodies (HcAbs) (1,2). Nbs contain four constant regions, named framework regions (FRs), and three connecting variable regions, called complementarity determining regions (CDRs). FRs are responsible for maintaining the structural integrity of Nbs, while CDRs directly bind to antigen epitopes (3). On the one hand, because of their nanometer size (~2.5 nm × 4 nm) and single domain structure, Nbs have the following advantages as antiviral agents: they can be easily expressed for bulk production, they are robust for convenient storage and transportation, and they have good permeability in tissues (4-6). On the other hand, also because of their small size, Nbs have the following potential limitations as antiviral agents: they may have limited binding affinity for antigens, and may be cleared from the body relatively quickly (the upper size limit of proteins for renal clearance is 60 kDa) (7,8). Nevertheless, the use of Nbs as antiviral therapeutic agents is gaining more and more clinical acceptance, with the focus on overcoming their potential limitations (9-11).

Middle East respiratory syndrome (MERS) coronavirus (MERS-CoV) was first identified in June 2012 (12) and continues to infect humans: it has led to at least 2,220 confirmed cases and 790 deaths (~36% fatality rate) in 27 countries (http://www.who.int/emergencies/mers-cov/en/). Bats and dromedary camels are likely the natural reservoir and transmission hosts, respectively, for MERS-CoV. Whereas camel-to-human transmission of MERS-CoV has accounted for most of the human infections, human-to-human spread of MERS-CoV also occurs sporadically (13,14). Currently, no therapeutic agents or vaccines have been approved for human use. Due to the continued threat of MERS-CoV, there is an urgent need to develop highly potent, cost-effective,

and broad-spectrum anti-MERS-CoV therapeutics and vaccines with the potential for large-scale industrial production.

Therapeutic antibodies have been shown to be effective antiviral agents (15,16). The receptor-binding domain (RBD) of MERS-CoV spike (S) protein is a prime target for therapeutic antibodies. The MERS-CoV S protein guides viral entry into host cells. It first binds to its host receptor dipeptidyl peptidase 4 (DPP4) through the RBD of its S1 subunit, and then fuses viral and host membranes through its S2 subunit (15,17-22). The RBD contains a receptor-binding motif (RBM) region (residues 484-567) that directly interacts with DPP4. We have previously shown that RBD-based vaccines are highly immunogenic and can induce the production of potent anti-MERS-CoV cross-neutralizing antibodies (23-27). Moreover, we have discovered several RBD-specific monoclonal antibodies (mAbs) with strong neutralizing activities against lethal MERS-CoV infections in human DPP4-transgenic (hDPP4-Tg) mice (15,28,29). These and some other RBD-targeting mAbs are currently being developed as anti-MERS-CoV therapeutics in experimental animal models (15,30-36). However, the widespread use of conventional antibodies can be limited by their large size, high production costs, inconvenient storage and transportation, and poor pharmacokinetics (37), making Nbs attractive alternatives to traditional mAbs to treat MERS-CoV infections. Currently, it has not been shown whether MERS-CoV RBD can reliably trigger the production of Nbs, whether the produced Nbs can overcome the potential limitations (e.g., low binding affinity for the RBD and relatively short half-life in the body), or whether the produced Nbs can demonstrate sufficient therapeutic efficacy to warrant further development in clinical settings.

Here after immunizing llama with recombinant MERS-CoV RBD protein, we generated a novel neutralizing Nb, NbMS10, and also constructed its human-Fc-fused version, NbMS10-Fc.

We further investigated these Nbs for their RBD-binding capabilities, neutralization mechanisms, cross-neutralizing activity against divergent MERS-CoV strains, half-life, and protective efficacy against lethal MERS-CoV infection in an established hDPP4-Tg mouse model (38). This study reveals that efficacious, robust and broad-spectrum Nbs can be produced to target MERS-CoV S protein RBD and that they hold great promise as potential anti-MERS-CoV therapeutics.

Results

Identification and characterization of MERS-CoV-RBD-specific Nbs.

To construct the Nb (i.e. VHH) library, we immunized llama with recombinant MERS-CoV RBD (residues 377-588, EMC2012 strain) containing a C-terminal human IgG1 Fc tag (i.e., RBD-Fc) and isolated peripheral blood mononuclear cells (PBMCs) from the immunized llama. After four rounds of bio-panning and screening using MERS-CoV RBD-Fc, we isolated a positive clone with the highest binding affinity for the RBD. The gene encoding this RBD-specific Nb was subcloned into yeast expression vector to construct NbMS10 (which contains a C-terminal His_6 tag) and NbMS10-Fc (which contains a C-terminal human IgG1 Fc tag) Nbs (Fig. 1). Both NbMS10 and NbMS10-Fc were expressed in yeast cells, secreted into the cell culture supernatants, and purified to homogeneity (Fig. 2A, left). The estimated molecular weights were about 16 kDa for NbMS10 and 50 kDa for NbMS10-Fc, since the latter formed a dimer. These MERS-CoV RBD-specific Nbs from llama, but not severe acute respiratory syndrome coronavirus (SARS-CoV) RBD-specific mAb from mice, were recognized by anti-llama antibodies (Fig. 2A, right). Thus, the yeast-expressed Nbs maintained their native conformation and antigenicity.

To characterize their functions, we examined how the Nbs interact with MERS-CoV RBDs. First, we evaluated the binding between the Nbs and MERS-CoV RBD using ELISA. The result

showed that both Nbs bound strongly to recombinant MERS-CoV RBD containing a C-terminal folden tag (RBD-Fd) and MERS-CoV S1 containing a C-terminal His_6 tag (S1-His) in a dose-dependent manner (Fig. 2B). Second, we determined the binding affinity of the two Nbs for MERS-CoV RBD using surface plasmon resonance (SPR). The result showed that the K_d between NbMS10 and RBD-Fc was 0.87 nM, whereas the K_d between NbMS10-Fc and S1-His was 0.35 nM (Fig. 2C). Third, we carried out MERS-CoV neutralization assay. The result showed that the Nbs efficiently neutralized the infection of live MERS-CoV (EMC2012 strain) in Vero cells. The measured 50% neutralization doses (ND_{50}) were 3.52 μg/ml for NbMS10 and 2.33 μg/ml for NbMS10-Fc (Fig. 2D). Taken together, the Nbs strongly bound to MERS-CoV RBD and neutralized MERS-CoV infection.

Molecular mechanism underlying the neutralizing activities of Nbs.

To investigate the mechanism underlying the neutralizing activities of Nbs, we evaluated the competition between the Nbs and hDPP4 for the binding to MERS-CoV RBD. First, we carried out a flow cytometry assay where recombinant MERS-CoV RBD interacted with cell-surface-expressed DPP4 in the presence or absence of recombinant Nbs. The result showed that both Nbs significantly blocked the binding of RBD to cell-surface DPP4 in a dose-dependent manner (Fig. 3A and B). As a negative control, SARS-CoV-RBD-specific 33G4 mAb did not block the binding between MERS-CoV RBD and cell-surface DPP4 (Fig. 3A and B). Second, we carried out an ELISA where recombinant MERS-CoV RBD and recombinant hDPP4 interacted in the presence or absence of recombinant Nbs. The result showed that both Nbs, but not 33G4 mAb, blocked the binding between MERS-CoV RBD and DPP4 in a dose-dependent manner. Moreover, compared to NbMS10, NbMS10-Fc blocked the RBD-DPP4 binding more efficiently (Fig. 3C). These data

reveal that the Nbs can compete with hDPP4 for the binding to MERS-CoV RBD, suggesting that the Nb-binding site and the DPP4-binding site overlap on the MERS-CoV RBD.

To map the binding site of the Nbs on MERS-CoV RBD, we performed alanine scanning on the surface of MERS-CoV RBD and detected the binding of Nbs to the alanine-containing RBD mutants. The results showed that NbMS10 demonstrated tight binding to MERS-CoV RBD containing the single mutations L506A, D510A, R511A, E513A, E536A, W553A, V555A, and E565A and slightly reduced binding to RBD containing triple mutations L506F-D509G-V534A, suggesting that these RBD residues do not play significant roles in Nb binding. Instead, single mutation D539A and double mutations E536A-D539A on MERS-CoV RBD both ablated the binding of NbMS10 to the RBD (Fig. 4A), suggesting that RBD residue Asp539 plays an important role in Nb binding. We further investigated the role of Asp539 in Nb binding using the MERS-CoV pseudovirus entry assay. Neither NbMS10 nor NbMS10-Fc could neutralize the cell entry of MERS-CoV pseudovirus bearing the D539A mutation, again confirming that residue Asp539 is critical for Nb binding (Fig. 4B). To examine of the role of the D539A mutation in DPP4 binding, we carried out an ELISA to detect the binding between DPP4 and MERS-CoV RBD bearing the D539A mutation. The result showed that the D539A mutation significantly reduced the binding of the RBD to DPP4 (Fig. 4C). Overall, these results demonstrate that Nbs recognize the Asp539-containing epitope on MERS-CoV RBD, and that this epitope also plays an important role in DPP4 binding. Therefore, the Nbs and DPP4 compete for the same region on MERS-CoV RBD, and mutations in this region can reduce the binding of both the Nbs and DPP4.

To investigate whether Nb-recognized epitopes on MERS-CoV RBD are conformational or linear, we detected the binding of Nbs to MERS-CoV RBD with its conformational structure disrupted. To this end, we treated MERS-CoV RBD with reducing agent DTT to break the

177 disulfide bonds in the protein, and performed an ELISA on the binding between Nbs and DTT-
178 treated RBD. The result showed that neither NbMS10 nor NbMS10-Fc bound to the DTT-treated
179 RBD (Fig. 4D). As a control, both Nbs bound to untreated RBD with high affinity. Thus, the Nbs
180 recognize the conformational epitope on the RBD.

181 To understand the structural mechanism underlying the neutralizing activities of the Nbs, we
182 examined the competitive interactions among the Nbs, DPP4, and MERS-CoV RBD using
183 structural modeling (Fig. 5**)**. In the absence of the Nbs, MERS-CoV RBD binds tightly to the DPP4
184 receptor, with D539 of RBD serving as a key residue at the binding interface (Fig. 5A). Here, RBD
185 residue D539 forms a critical salt bridge with DPP4, and it interacts with the surrounding key RBD
186 residues via van der Waals contacts and hydrogen bonds (Fig. 5B), enabling RBD and DPP4 to
187 maintain strong binding interactions. The Nbs bind tightly to the RBD in the same D539-
188 containing region, abolishing the binding between RBD and DPP4 (Fig. 5C).

189

190 **Cross-neutralizing activity of Nbs against divergent MERS-CoV strains.**

191 To investigate the cross-neutralizing activity of Nbs against divergent MERS-CoV isolates,
192 we performed MERS-CoV pseudovirus entry assay in the presence of the Nbs where the
193 pseudoviruses encode the S gene of various MERS-CoV isolates from different countries (Saudi
194 Arabia, Qatar, and South Korea), hosts (human and camels), and time periods (2012-2015). These
195 MERS-CoV strains all contain mutations in their RBD. The results showed that both Nbs potently
196 neutralized the cell entry of all of the MERS-CoV pseudoviruses, with the ND_{50} values ranging
197 from 0.003 to 0.979 μg/ml (for NbMS10) and from 0.003 to 0.067 μg/ml (for NbMS10-Fc) (Table
198 1). Therefore, although the Nbs were developed using the RBD from one MERS-CoV strain

(EMC2012), they have broad-spectrum cross-neutralizing activity against existing MERS-CoV strains as well as potentially future emerging MERS-CoV strains.

***In vivo* half-life of Nbs.**

To evaluate the *in vivo* half-life of the Nbs, we injected the Nbs into mice, collected the sera from the mice after different time intervals, and measured the binding between the sera and recombinant MERS-CoV S1 using ELISA. The results showed that the sera collected from NbMS10-injected mice gradually lost their binding affinity for MERS-CoV S1, and completely lost their binding for MERS-CoV S1 10 days post-injection (Fig. 6A). In comparison, NbMS10-Fc demonstrated stable binding for recombinant MERS-CoV S1 10 days post-injection (Fig. 6B). As a control experiment, sera collected from PBS-injected mice showed no binding for recombinant MERS-CoV S1 (Fig. 6C). Thus, compared to monomeric Nb, Fc-fused Nb has a significantly extended *in vivo* half-life likely due to its dimeric structure, which increases the molecular weight of Nb from 16 kDa to 50 kDa and hence may slow down its renal clearance.

Prophylactic and therapeutic efficacy of Nb in transgenic mice.

Because MERS-CoV does not infect wild-type mice, we previously developed hDPP4-Tg mice (38) as the susceptible animal model for MERS-CoV research. To evaluate the prophylactic efficacy of NbMS10-Fc, mice were injected with a single dose of NbMS10-Fc 3 days before they were infected with a lethal dose of MERS-CoV, and were subsequently monitored for their weight and survival. Trastuzumab, an antibody used for treating breast cancer, was used as a control. The result showed that after MERS-CoV infection, mice treated with NbMS10-Fc had a 100% survival rate (Fig. 7A, above) and steady weight (Fig. 7A, below). In comparison, mice treated with

trastuzumab all died on the 8th day post-infection and their weight also sharply decreased starting from the 4th day post-infection (Fig. 7A). To evaluate the therapeutic efficacy of NbMS10-Fc, mice were first infected with MERS-CoV and then treated with single-dose NbMS10-Fc either 1 day or 3 days post-infection. The result showed that mice treated with NbMS10-Fc on the 1st day post-infection had a 100% survival rate and steady weight (Fig. 7B). In addition, mice treated with NbMS10-Fc on the 3rd day post-infection also had a 100% survival rate (Fig. 7C, above); although their weight first decreased on the 5th day post-infection, it rebounded on the 7th day post-infection (Fig. 7C, below). In comparison, mice receiving trastuzumab all died on day 8 after infection and their weight continuously decreased (Fig. 7B and C). Overall, NbMS10-Fc has potent prophylactic and therapeutic efficacy in protecting susceptible animal models against lethal MERS-CoV challenge.

Discussion

MERS-CoV continues to infect humans with a high fatality rate. Because camels likely serve as the transmission hosts for MERS-CoV and also because humans have contact with camels, the constant and continuing transmissions of MERS-CoV from camels to humans make it difficult to eradicate MERS-CoV from the human population. Thus, efficacious, cost-effective, and broad-spectrum anti-MERS-CoV therapeutic agents are needed to prevent and treat MERS-CoV infections in both humans and camels. Nbs have been gaining acceptance as antiviral agents because of their small size, good tissue permeability, and cost-effective production, storage, and transportation. However, their small size may also lead to relative low antigen-binding affinity and quick clearance from the host body. In this study, we have developed a novel MERS-CoV-

targeting Nb, NbMS10, and its Fc-fused version, NbMS10-Fc, both of which demonstrate great promise as anti-MERS-CoV therapeutic agents.

NbMS10 and NbMS10-Fc present superior characteristics common to other Nbs. They target the MERS-CoV RBD, which plays an essential role in cell entry of MERS-CoV by binding to its receptor hDPP4. Both Nbs can be expressed in yeast cells with high purity and yields, and are soluble in solutions. All of these properties suggest cost-effective production, easy storage, and convenient transportation of these Nbs in potential commercial applications.

The MERS-CoV RBD-targeting Nbs developed also demonstrate good qualities comparable to previously reported MERS-CoV RBD-specific conventional IgGs. First, the Nbs bind to MERS-CoV RBD with high affinities. The K_d values for NbMS10 and NbMS10-Fc to bind MERS-CoV RBD were 8.71×10^{-10} M and 3.46×10^{-10} M, respectively. The K_d values for RBD-targeting conventional IgGs to bind MERS-CoV RBD range from 7.12×10^{-8} M to 4.47×10^{-11} M (29,35,36). Moreover, the ND_{50} values for NbMS10 and NbMS10-Fc to neutralize MERS-CoV (EMC2012 strain) infection in cultured cells were 3.52 and 2.33 μg/ml, respectively. The ND_{50} values for RBD-specific conventional IgGs to neutralize various MERS-CoV strains ranged from microgram/ml to nanogram/ml (30,32,35,39,40). Thus, the Nbs developed in this study and conventional IgGs reported previously have comparable MERS-CoV RBD-binding affinities and MERS-CoV-neutralizing activities. Structural comparisons of conventional IgGs and Nbs have shown that the antigen-binding site of IgGs consists of paired heavy-chain and light-chain variable (VH-VL) domains, whereas Nbs lack the light chain and hence cannot form the paired VH-VL domains (8,41). Instead, Nbs have an extended CDR3 region (>16 amino acid residues), longer than that of the VHs of conventional IgGs (average length 12 amino acid residues) (42-44). Moreover, the Nbs developed here contain a 22-amino-acid CDR3; the extended CDR3 enables the

267 Nbs to bind to the antigens with higher affinity (37). Furthermore, although the single-domain Nb
268 (i.e., NbMS10) is small and can be cleared from the serum relatively quickly, the Fc-fused Nb (i.e.,
269 NbMS10-Fc) with relatively increased size demonstrates extended *in vivo* half-life. Therefore, the
270 potential short half-life of Nbs can be overcome by adding the appropriate tag to the Nbs to
271 increase their half-life. Overall, the current study has shown the feasibility of overcoming the
272 potential limitations of Nbs.

273 The MERS-CoV RBD-targeting Nbs potently neutralize MERS-CoV entry into host cells. The
274 K_d values between the Nbs and MERS-CoV RBD are significantly lower than that between MERS-
275 CoV RBD and hDPP4 receptor. As a result, the Nbs can outcompete hDPP4 for the binding of
276 MERS-CoV RBD, thereby blocking the binding of MERS-CoV to DPP4 as well as MERS-CoV
277 entry into host cells. It is worth noting that the RBD on the MERS-CoV S trimer frequently
278 undergoes conformational changes, switching between a lying down, receptor-inaccessible
279 conformation and a standing up, receptor-accessible conformation. Hence, in the context of the
280 virus particles where the RBD is part of the S protein, the Nbs would need to bind the RBD when
281 the RBD is in the standing up conformation (45). Importantly, the Nbs demonstrate strong cross-
282 neutralizing activities against various MERS-CoV strains isolated from different hosts (humans
283 and camels) and from different time points during MERS-CoV circulation in humans (from years
284 2012 to 2015). NbMS10 had a relatively high ND_{50} against AGV08584/2012 strain containing a
285 V534A mutation, consistent with the slightly reduced binding affinity between NbMS10 and
286 MERS-CoV RBD containing the V534A mutation (Fig. 4A). The broad neutralizing spectrum of
287 the Nbs results from the binding site of the Nbs on MERS-CoV RBD, which is located in the
288 Asp539-containing region that plays a critical role in DPP4 binding. Interestingly, several MERS-
289 CoV RBD-specific conventional IgGs also bind to the same epitope (39,46), suggesting that this

region is a hot spot for immune recognition. Although mutations in this region can eliminate the binding of the Nbs to MERS-CoV RBD and hence lead to viral immune evasion, they also reduce the binding of MERS-CoV RBD to receptor DPP4 and hence decrease the efficiency of viral entry. Thus, viral immune evasion from the inhibition of the Nbs through mutations can be costly to MERS-CoV itself. Indeed, residue Asp539 in S protein RBD is highly conserved in almost all of the natural MERS-CoV strains published to date (Fig. 8). Therefore, the MERS-CoV-specific Nbs can potentially be developed into broad-spectrum anti-MERS-CoV therapeutic agents. Despite the above analysis, this study did not examine all possible mutations in the Nb-binding region (since the atomic structures of MERS-CoV RBD complexed with the Nbs are still unknown), and thus it is possible that future escape mutations may occur to residues that this study did not cover. In that case, a combination of the current Nbs and other antibodies targeting other S regions or various RBD epitopes may be helpful in battling the emergence of immune escape MERS-CoV strains.

In sum, the MERS-CoV-specific Nbs developed in the current study possess superior qualities common to all Nbs such as their small size and cost-effective production. They also overcome potential limitations of other Nbs by maintaining high binding affinity for their target MERS-CoV RBD and optimized half-life. Moreover, they recognize a functionally important region on MERS-CoV RBD, rendering viral immune evasion costly and at the same time making themselves good candidates as broad-spectrum anti-MERS-CoV therapeutics. We have confirmed the effectiveness of the Nbs by showing that the Fc-fused Nb completely protected animal models from lethal MERS-CoV challenge. Thus, the Nbs can potentially be used in both humans and camels to prevent and treat MERS-CoV infections in either of these hosts and also block the camel-to-human transmission of MERS-CoV. Overall, our study proves the feasibility of developing highly

effective Nbs as anti-MERS-CoV therapeutic agents, and points out strategies to preserve the advantages of Nbs as well as to overcome the potential limitations of Nbs.

Materials and Methods

Ethics statement. The animal studies were carried out in strict accordance with the recommendations in the Guide for the Care and Use of Laboratory Animals of the State Key Laboratory of Pathogen and Biosecurity at the Beijing Institute of Microbiology and Epidemiology of China and the National Institutes of Health (NIH). The animal protocols were approved by the IACUC of the State Key Laboratory of Pathogen and Biosecurity, Beijing Institute of Microbiology and Epidemiology (Permit number: BIME 2015-0024) and by the Committee on the Ethics of Animal Experiments of the New York Blood Center (Approval Number: 194.18).

Construction of VHH library and screening for MERS-CoV-RBD-specific Nbs. Construction of the Nb (i.e., VHH) library and screening of MERS-CoV-RBD-specific Nbs were performed as previously described (47). Briefly, male and female alpaca (llama pacos, one year) were subcutaneously (s.c.) immunized with recombinant RBD-Fc (260 μg/alpaca) (48) plus Freund's complete adjuvant, and boosted three times with the same immunogen plus Freund's incomplete adjuvant (InvivoGen). Blood was collected 10 days post-last immunization and then PBMCs were isolated using Ficoll-Paque gradient centrifugation (GE Healthcare). Total RNA was extracted with TRIzol reagent (Invitrogen). cDNA was synthesized by reverse transcription (RT)-PCR using TransScript cDNA Synthesis SuperMix (TransGen Biotech, China), followed by PCR amplification of the N-terminal IgG heavy-chain fragment (~700 bp), using forward primer VHH-L-F (5'-GGTGGTCCTGGCTGC-3') and reverse primer CH2-R (5'-

GGTACGTGCTGTTGAACTGTTCC-3'). The VHH gene (~300-450 bp) was further amplified using the above DNA fragment as template and forward primer VHH-FR1-D-F (5'-TTTCTATTACTAGGCCCAGCCGGCCGAGTCTGGAGGRRGCTTGGTGCA-3') and reverse primer VHH-FR4-D-R (5'-AAACCGTTGGCCATAATGGCCTGAGGAGACGRTGACSTSGG TC-3') (*Sfi*I restriction site underlined). The *Sfi*I-digested VHH DNA fragment was then inserted into phagemid vector pCANTAB5e (Bio-View Shine Biotechnology, China) to construct the VHH phage display library (49). Phage particles were analyzed by ELISA using recombinant MERS-CoV RBD-Fc and Fc of human IgG1 proteins as the positive and negative target proteins, respectively, to screen for RBD-specific Nbs. After four rounds of bio-panning, one of five positive clones, CAb10, with the highest binding to MERS-CoV RBD, was selected for further analyses (Fig. 1).

Expression of MERS-CoV-RBD-specific Nbs in yeast cells. NbMS10 and NbMS10-Fc Nbs containing a C-terminal His_6 and Fc of human IgG1, respectively, were constructed based on the aforementioned CAb10 VHH. The DNA sequences encoding NbAb10 and NbAb10-Fc were synthesized (GenScript) and inserted into *Pichia* pastoris secretory expression vector, pPICZαA (Invitrogen) (Fig. 1). The recombinant NbMS10 and NbMS-Fc were expressed in *Pichia pastoris* GS115 cells, and purified using a Ni-NTA column (for NbMS10) (GE Healthcare) and a protein A Sepharose 4 Fast Flow column (for NbMS10-Fc) (GE Healthcare), respectively.

SDS-PAGE and Western blot. The purified anti-MERS-CoV-RBD Nbs were analyzed using SDS-PAGE and Western blot (23,48). Briefly, Nbs (3 μg) were loaded to 10% Tris-Glycine SDS-PAGE gels and stained for Coomassie Brilliant Blue, or transferred to nitrocellulose membranes.

After being blocked overnight at 4°C with 5% non-fat milk-PBST (5% PBST), the membranes were incubated sequentially with goat anti-llama IgG (1:3,000) (Abcam), horseradish peroxidase (HRP)-conjugated anti-goat IgG (1:1,000) antibodies (R&D Systems) for 1 h at room temperature, and then ECL Western blot substrate reagents. Finally, the membranes were visualized using Amersham Hyperfilm (GE Healthcare). SARS-CoV-RBD-specific mAb, 33G4 (50), was used as a control.

ELISA. ELISA was performed to detect the binding between Nbs and MERS-CoV S1 or RBD proteins (23,51). Briefly, ELISA plates were coated overnight at 4°C respectively with recombinant MERS-CoV S1-His (48), RBD-Fc (48), RBD-Fd (51), or one of the mutant RBDs containing a C-terminal human Fc tag (28). After being blocked with 2% PBST for 2 h at 37°C, the plates were further incubated sequentially with serially diluted Nbs (containing a C-terminal His_6 or Fc tag), either goat anti-llama (1:5,000) or mouse anti-His (1:3,000) antibody (Sigma), and either HRP-conjugated anti-goat IgG (1:3,000) or anti-mouse IgG (1:5,000) antibody (GE Healthcare) for 1 h at 37°C. ELISA substrate (3,3′,5,5′-tetramethylbenzidine: TMB, Invitrogen) was added to the plates, and the reactions were stopped with 1N H_2SO_4. Absorbance at 450 nm (A450) was measured using Tecan Infinite 200 PRO Microplate Reader (Tecan).

To detect the binding between Nbs and denatured MERS-CoV RBD protein, ELISA plates were coated with RBD-Fd protein (2 μg/ml) overnight at 4°C, and then sequentially incubated with dithiothreitol (DTT) (10 mM) and iodoacetamide (50 mM) (Sigma) for 1 h at 37°C (28). After three washes using PBST, ELISA was performed as described above.

Inhibition of the binding between MERS-CoV RBD and hDPP4 proteins by Nbs was performed using ELISA as described above, except that recombinant hDPP4 protein (2 μg/ml)

(R&D Systems) and serially diluted Nbs were added simultaneously to the RBD-Fc-coated plates. The binding between RBD and DPP4 was detected using goat anti-hDPP4 antibody (1:1,000) (R&D Systems) and HRP-conjugated anti-goat IgG (1:3,000). % inhibition was calculated based on the A450 values of RBD-hDPP4 binding in the presence and absence of Nbs. SARS-CoV 33G4 mAb was used as a negative control to Nbs.

Surface plasmon resonance (SPR). The binding between Nbs and MERS-CoV S1 or RBD protein was detected using a BiacoreS200 instrument (GE Healthcare) as previously described (29). Briefly, recombinant Fc-fused MERS-CoV RBD-Fc protein or NbMS10-Fc Nb (5 μg/ml) was captured on a Sensor Chip Protein A (GE Healthcare), and recombinant His_6-tagged MERS-CoV S1-His protein or NbMS10 Nb at various concentrations was flown over the chip surface in a running buffer containing 10 mM HEPES, pH 7.4, 150 mM NaCl, 3 mM EDTA, and 0.05% surfactant P20. The sensorgram was analyzed using Biacore S200 software, and the data were fitted to a 1:1 binding model.

Flow cytometry. This assay was performed to detect the inhibition of the binding between MERS-CoV RBD and cell-surface hDPP4 by Nbs (28). Briefly, Huh-7 cells expressing hDPP4 were incubated with MERS-CoV RBD-Fc protein (20 μg/ml) for 30 min at room temperature in the absence or presence of Nbs at various concentrations. Cells were incubated with FITC-labeled anti-human IgG antibody (1:50, Sigma) for 30 min, and then analyzed by flow cytometry. % inhibition was calculated based on the fluorescence intensity of RBD-Huh-7 cell binding in the presence and absence of Nbs.

404 **MERS pseudovirus neutralization assay.** Neutralization of MERS pseudovirus entry by Nbs was
405 performed as previously described (23,52). Briefly, 293T cells were cotransfected with a plasmid
406 encoding Env-defective, luciferase-expressing HIV-1 genome (pNL4-3.luc.RE) and a plasmid
407 encoding MERS-CoV S protein. The MERS pseudoviruses were harvested from supernatants 72 h
408 post-transfection, and then incubated with Nbs at 37°C for 1 h before being added to Huh-7 cells.
409 After 72 h, the cells were lysed in cell lysis buffer (Promega), incubated with luciferase substrate
410 (Promega), and assayed for relative luciferase activity using Tecan Infinite 200 PRO Luminator
411 (Tecan). The ND_{50} of Nbs was calculated as previously described (53).
412
413 **MERS-CoV micro-neutralization assay.** Neutralization of MERS-CoV infection by Nbs was
414 performed as previously described (28,54). Briefly, MERS-CoV (EMC2012 strain) at an amount
415 equal to 100 $TCID_{50}$ was incubated with Nbs at different concentrations for 1 h at 37°C. Then the
416 Nb-virus mixture was incubated with Vero E6 cells for 72 h at 37°C in the presence of 5% CO_2.
417 The CPE was observed daily. The neutralizing activity of Nbs was reported as ND_{50}. The Reed-
418 Muench method was used to calculate the values of ND_{50} for each Nb (55).
419
420 **Measurement of half-life of Nbs.** Male and female C57BL/6 mice (6-8-week-old) were
421 intravenously (i.v.) injected with Nbs (50 μg in 200 μl per mouse) into the tail vein. Sera were
422 collected at different time points (30 min, 2 h, 6 h, 1-, 5- and 10-day post-injection). The
423 concentrations of Nbs in the sera were detected by ELISA, as described above. Briefly, MERS-
424 CoV S1-His protein (2 μg/ml) was used to coat ELISA plates, and then sera, goat anti-llama
425 (1:5,000), and HRP-conjugated anti-goat IgG (1:3,000) antibodies were sequentially added for
426 ELISA reactions.

427

428 **Evaluation of protective efficacy of NbMS10-Fc Nb.** The prophylactic and therapeutic efficacy
429 of NbMS10-Fc was evaluated in hDPP4-Tg mice as previously described (29). Briefly, male and
430 female mice (8-10-week-old) were intraperitoneally (i.p.) anesthetized with sodium pentobarbital
431 (5 mg/kg of body weight) before being intranasally (i.n.) inoculated with lethal dose of MERS-
432 CoV (EMC2012 strain, $10^{5.3}$ $TCID_{50}$) in 20 µl of Dulbecco's modified Eagle's medium (DMEM).
433 Either 3 days pre-infection or 1 or 3 days post-infection, mice were i.p. injected with NbMS10-Fc
434 (10 mg/kg). Trastuzumab mAb was used as a control to Nbs. The infected mice were observed
435 daily for 14 days, and their body weights and survivals were recorded.

436

437 **Statistical analysis.** Statistical analysis was performed using GraphPad Prism version 5.01. To
438 compare the binding of Nbs to MERS-CoV S1 or RBD protein, as well as the RBDs with or
439 without D539A mutation to hDPP4 receptor, two tailed Student's *t* test was used. One-way
440 ANOVA was used to compare the inhibition of Nbs to RBD-hDPP4 binding. Statistical
441 significance between survival curves was analyzed using Kaplan-Meier survival analysis with a
442 log-rank test. *P* values lower than 0.05 were considered statistically significant. *, ** and ***
443 indicate $P < 0.05$, $P < 0.01$, and $P < 0.001$, respectively.

444

445 **Data availability**

446 All data needed to evaluate the conclusions in the paper are present in the paper. Additional data
447 related to this paper may be requested from the authors.

448

449

Acknowledgments

This study was supported by the National Key Plan for Scientific Research and Development of China 2016YFD0500306, NSFC81571983, Technology Innovation Fund in China 3407049, the State Key Laboratory of Pathogen and Biosecurity grant SKLPBS1704 (to G.Z. and Y.Z.), NIH grants R01AI137472, R21AI109094, and R21AI128311 (to S.J. and L.D), NIH grants R01AI089728 and R01AI110700 (to F.L.), and NIH grant R01AI139092 (to S.J., F.L., and L.D.).

The funders had no role in study design, data collection and interpretation, or the decision to submit the work for publication.

The authors declare no competing interests.

G.Z., L.D., and Y.Z. designed the study. G.Z., L.H., S.S., H.Q., W.T., J.C., J.L., Y.C., Y.G., Y.W, K.J, R.F., and E.D. performed the experiments. G.Z, W.T., S.J., L.D. and Y.Z. summarized and analyzed the data. J.S. and F.L. performed the structural analysis. G.Z., F.L., L.D., and Y.Z. wrote the manuscript. S.J., F.L., L.D., and Y.Z. revised the manuscript.

References

1. Konning D, Zielonka S, Grzeschik J, Empting M, Valldorf B, Krah S, Schroter C, Sellmann C, Hock B, Kolmar H. 2017. Camelid and shark single domain antibodies: structural features and therapeutic potential. Curr Opin Struct Biol 45:10-16.

2. De MT, Muyldermans S, Depicker A. 2014. Nanobody-based products as research and diagnostic tools. Trends Biotechnol 32:263-270.

3. Noel F, Malpertuy A, de Brevern AG. 2016. Global analysis of VHHs framework regions with a structural alphabet. Biochimie 131:11-19.

4. Wilken L, McPherson A. 2017. Application of camelid heavy-chain variable domains (VHHs) in prevention and treatment of bacterial and viral infections. Int Rev Immunol 37:69-76.

5. Van HG, Allosery K, De B, V, De ST, Detalle L, de FA. 2017. Nanobodies(R) as inhaled biotherapeutics for lung diseases. Pharmacol Ther 169:47-56.

6. Detalle L, Stohr T, Palomo C, Piedra PA, Gilbert BE, Mas V, Millar A, Power UF, Stortelers C, Allosery K. 2015. Generation and characterization of ALX-0171, a potent novel therapeutic nanobody for the treatment of respiratory syncytial virus infection. Antimicrob Agents Chemother 60:6-13.

7. Steeland S, Vandenbroucke RE, Libert C. 2016. Nanobodies as therapeutics: big opportunities for small antibodies. Drug Discov Today 21:1076-1113.

8. Muyldermans S. 2013. Nanobodies: natural single-domain antibodies. Annu Rev Biochem 82:775-797.

9. Peyvandi F, Scully M, Kremer Hovinga JA, Cataland S, Knobl P, Wu H, Artoni A, Westwood JP, Mansouri TM, Jilma B. 2016. Caplacizumab for acquired thrombotic thrombocytopenic purpura. N Engl J Med 374:511-522.

10. Keyaerts M, Xavier C, Heemskerk J, Devoogdt N, Everaert H, Ackaert C, Vanhoeij M, Duhoux FP, Gevaert T, Simon P. 2016. Phase I study of 68Ga-HER2-nanobody for PET/CT assessment of HER2 expression in breast carcinoma. J Nucl Med 57:27-33.

11. Holz JB. 2012. The TITAN trial--assessing the efficacy and safety of an anti-von Willebrand factor Nanobody in patients with acquired thrombotic thrombocytopenic purpura. Transfus Apher Sci 46:343-346.

12. Zaki AM, van BS, Bestebroer TM, Osterhaus AD, Fouchier RA. 2012. Isolation of a novel coronavirus from a man with pneumonia in Saudi Arabia. N Engl J Med 367:1814-1820.

13. Omrani AS, Al-Tawfiq JA, Memish ZA. 2015. Middle East respiratory syndrome coronavirus (MERS-CoV): animal to human interaction. Pathog Glob Health 109:354-362.

499 14.Lau SKP, Wong ACP, Lau TCK, Woo PCY. 2017. Molecular evolution of MERS Coronavirus:
500 dromedaries as a recent intermediate host or long-time animal reservoir? Int J Mol Sci 18. pii:
501 E2138.

502 15. Du L, Yang Y, Zhou Y, Lu L, Li F, Jiang S. 2017. MERS-CoV spike protein: a key target for
503 antivirals. Expert Opin Ther Targets 21:131-143.

504 16. Wang Q, Wong G, Lu G, Yan J, Gao GF. 2016. MERS-CoV spike protein: Targets for
505 vaccines and therapeutics. Antiviral Res 133:165-177.

506 17. Li F. 2015. Receptor recognition mechanisms of coronaviruses: a decade of structural studies. J
507 Virol 89:1954-1964.

508 18. Lu L, Liu Q, Zhu Y, Chan KH, Qin L, Li Y, Wang Q, Chan JF, Du L, Yu F. 2014. Structure-
509 based discovery of Middle East respiratory syndrome coronavirus fusion inhibitor. Nat
510 Commun 5:3067.

511 19. Lu G, Hu Y, Wang Q, Qi J, Gao F, Li Y, Zhang Y, Zhang W, Yuan Y, Bao J. 2013. Molecular
512 basis of binding between novel human coronavirus MERS-CoV and its receptor CD26. Nature
513 500:227-231.

514 20. Wang N, Shi X, Jiang L, Zhang S, Wang D, Tong P, Guo D, Fu L, Cui Y, Liu X. 2013.
515 Structure of MERS-CoV spike receptor-binding domain complexed with human receptor DPP4.
516 Cell Res 23:986-993.

517 21. Raj VS, Mou H, Smits SL, Dekkers DH, Muller MA, Dijkman R, Muth D, Demmers JA, Zaki
518 A, Fouchier RA. 2013. Dipeptidyl peptidase 4 is a functional receptor for the emerging human
519 coronavirus-EMC. Nature 495:251-254.

520 22. Li F. 2016. Structure, function, and evolution of coronavirus spike proteins. Annu Rev Virol
521 3:237-261.

522 23. Tai W, Wang Y, Fett CA, Zhao G, Li F, Perlman S, Jiang S, Zhou Y, Du L. 2017.
523 Recombinant receptor-binding domains of multiple Middle East respiratory syndrome

coronaviruses (MERS-CoVs) induce cross-neutralizing antibodies against divergent human and camel MERS-CoVs and antibody escape mutants. J Virol 91. pii: e01651-16.

24. Ma C, Li Y, Wang L, Zhao G, Tao X, Tseng CT, Zhou Y, Du L, Jiang S. 2014. Intranasal vaccination with recombinant receptor-binding domain of MERS-CoV spike protein induces much stronger local mucosal immune responses than subcutaneous immunization: Implication for designing novel mucosal MERS vaccines. Vaccine 32:2100-2108.

25. Zhang N, Channappanavar R, Ma C, Wang L, Tang J, Garron T, Tao X, Tasneem S, Lu L, Tseng CT. 2016. Identification of an ideal adjuvant for receptor-binding domain-based subunit vaccines against Middle East respiratory syndrome coronavirus. Cell Mol Immunol 13:180-190.

26. Du L, Tai W, Zhou Y, Jiang S. 2016. Vaccines for the prevention against the threat of MERS-CoV. Expert Rev Vaccines 15:1123-1134.

27. Du L, Tai W, Yang Y, Zhao G, Zhu Q, Sun S, Liu C, Tao X, Tseng CK, Perlman S. 2016. Introduction of neutralizing immunogenicity index to the rational design of MERS coronavirus subunit vaccines. Nat Commun 7:13473.

28. Du L, Zhao G, Yang Y, Qiu H, Wang L, Kou Z, Tao X, Yu H, Sun S, Tseng CT. 2014. A conformation-dependent neutralizing monoclonal antibody specifically targeting receptor-binding domain in Middle East respiratory syndrome coronavirus spike protein. J Virol 88:7045-7053.

29. Qiu H, Sun S, Xiao H, Feng J, Guo Y, Tai W, Wang Y, Du L, Zhao G, Zhou Y. 2016. Single-dose treatment with a humanized neutralizing antibody affords full protection of a human transgenic mouse model from lethal Middle East respiratory syndrome (MERS)-coronavirus infection. Antiviral Res 132:141-148.

30. Corti D, Zhao J, Pedotti M, Simonelli L, Agnihothram S, Fett C, Fernandez-Rodriguez B, Foglierini M, Agatic G, Vanzetta F. 2015. Prophylactic and postexposure efficacy of a potent human monoclonal antibody against MERS coronavirus. Proc Natl Acad Sci U S A 112:10473-10478.

31. Pascal KE, Coleman CM, Mujica AO, Kamat V, Badithe A, Fairhurst J, Hunt C, Strein J, Berrebi A, Sisk JM. 2015. Pre- and postexposure efficacy of fully human antibodies against Spike protein in a novel humanized mouse model of MERS-CoV infection. Proc Natl Acad Sci U S A 112:8738-8743.

32. Li Y, Wan Y, Liu P, Zhao J, Lu G, Qi J, Wang Q, Lu X, Wu Y, Liu W. 2015. A humanized neutralizing antibody against MERS-CoV targeting the receptor-binding domain of the spike protein. Cell Res 25:1237-1249.

33. Johnson RF, Bagci U, Keith L, Tang X, Mollura DJ, Zeitlin L, Qin J, Huzella L, Bartos CJ, Bohorova N. 2016. 3B11-N, a monoclonal antibody against MERS-CoV, reduces lung pathology in rhesus monkeys following intratracheal inoculation of MERS-CoV Jordan-n3/2012. Virology 490:49-58.

34. van DN, Falzarano D, Ying T, de WE, Bushmaker T, Feldmann F, Okumura A, Wang Y, Scott DP, Hanley PW. 2017. Efficacy of antibody-based therapies against Middle East respiratory syndrome coronavirus (MERS-CoV) in common marmosets. Antiviral Res 143:30-37.

35. Jiang L, Wang N, Zuo T, Shi X, Poon KM, Wu Y, Gao F, Li D, Wang R, Guo J. 2014. Potent neutralization of MERS-CoV by human neutralizing monoclonal antibodies to the viral spike glycoprotein. Sci Transl Med 6:234ra59.

36. Ying T, Du L, Ju TW, Prabakaran P, Lau CC, Lu L, Liu Q, Wang L, Feng Y, Wang Y. 2014. Exceptionally potent neutralization of middle East respiratory syndrome coronavirus by human monoclonal antibodies. J Virol 88:7796-7805.

37. Bannas P, Hambach J, Koch-Nolte F. 2017. Nanobodies and nanobody-based human heavy chain antibodies as antitumor therapeutics. Front Immunol 8:1603.

38. Zhao G, Jiang Y, Qiu H, Gao T, Zeng Y, Guo Y, Yu H, Li J, Kou Z, Du L. 2015. Multi-Organ damage in human dipeptidyl peptidase 4 transgenic mice infected with Middle East respiratory syndrome-coronavirus. PLoS One 10:e0145561.

575 39. Ying T, Prabakaran P, Du L, Shi W, Feng Y, Wang Y, Wang L, Li W, Jiang S, Dimitrov DS.
576 2015. Junctional and allele-specific residues are critical for MERS-CoV neutralization by an
577 exceptionally potent germline-like antibody. Nat Commun 6:8223.

578 40. Tang XC, Agnihothram SS, Jiao Y, Stanhope J, Graham RL, Peterson EC, Avnir Y, Tallarico
579 AS, Sheehan J, Zhu Q. 2014. Identification of human neutralizing antibodies against MERS-
580 CoV and their role in virus adaptive evolution. Proc Natl Acad Sci U S A 111:E2018-E2026.

581 41. Gonzalez-Sapienza G, Rossotti MA, Tabares-da RS. 2017. Single-domain antibodies as
582 versatile affinity reagents for analytical and diagnostic applications. Front Immunol 8:977.

583 42. Wesolowski J, Alzogaray V, Reyelt J, Unger M, Juarez K, Urrutia M, Cauerhff A, Danquah W,
584 Rissiek B, Scheuplein F. 2009. Single domain antibodies: promising experimental and
585 therapeutic tools in infection and immunity. Med Microbiol Immunol 198:157-174.

586 43. Muyldermans S. 2001. Single domain camel antibodies: current status. J Biotechnol 74:277-
587 302.

588 44. Chan PH, Pardon E, Menzer L, De GE, Kumita JR, Christodoulou J, Saerens D, Brans A,
589 Bouillenne F, Archer DB. 2008. Engineering a camelid antibody fragment that binds to the
590 active site of human lysozyme and inhibits its conversion into amyloid fibrils. Biochemistry
591 47:11041-11054.

592 45. Yuan Y, Cao D, Zhang Y, Ma J, Qi J, Wang Q, Lu G, Wu Y, Yan J, Shi Y. 2017. Cryo-EM
593 structures of MERS-CoV and SARS-CoV spike glycoproteins reveal the dynamic receptor
594 binding domains. Nat Commun 8:15092.

595 46. Yu X, Zhang S, Jiang L, Cui Y, Li D, Wang D, Wang N, Fu L, Shi X, Li Z. 2015. Structural
596 basis for the neutralization of MERS-CoV by a human monoclonal antibody MERS-27. Sci
597 Rep 5:13133.

598 47. Frenken LG, van der Linden RH, Hermans PW, Bos JW, Ruuls RC, de GB, Verrips CT. 2000.
599 Isolation of antigen specific llama VHH antibody fragments and their high level secretion by
600 Saccharomyces cerevisiae. J Biotechnol 78:11-21.

48. Ma C, Wang L, Tao X, Zhang N, Yang Y, Tseng CT, Li F, Zhou Y, Jiang S, Du L. 2014. Searching for an ideal vaccine candidate among different MERS coronavirus receptor-binding fragments--the importance of immunofocusing in subunit vaccine design. Vaccine 32:6170-6176.

49. Saerens D, Kinne J, Bosmans E, Wernery U, Muyldermans S, Conrath K. 2004. Single domain antibodies derived from dromedary lymph node and peripheral blood lymphocytes sensing conformational variants of prostate-specific antigen. J Biol Chem 279:51965-51972.

50. He Y, Lu H, Siddiqui P, Zhou Y, Jiang S. 2005. Receptor-binding domain of severe acute respiratory syndrome coronavirus spike protein contains multiple conformation-dependent epitopes that induce highly potent neutralizing antibodies. J Immunol 174:4908-4915.

51. Tai W, Zhao G, Sun S, Guo Y, Wang Y, Tao X, Tseng CK, Li F, Jiang S, Du L. 2016. A recombinant receptor-binding domain of MERS-CoV in trimeric form protects human dipeptidyl peptidase 4 (hDPP4) transgenic mice from MERS-CoV infection. Virology 499:375-382.

52. Zhao G, Du L, Ma C, Li Y, Li L, Poon VK, Wang L, Yu F, Zheng BJ, Jiang S. 2013. A safe and convenient pseudovirus-based inhibition assay to detect neutralizing antibodies and screen for viral entry inhibitors against the novel human coronavirus MERS-CoV. Virol J 10:266.

53. Chou TC. 2006. Theoretical basis, experimental design, and computerized simulation of synergism and antagonism in drug combination studies. Pharmacol Rev 58:621-681.

54. Wang Y, Tai W, Yang J, Zhao G, Sun S, Tseng CK, Jiang S, Zhou Y, Du L, Gao J. 2017. Receptor-binding domain of MERS-CoV with optimal immunogen dosage and immunization interval protects human transgenic mice from MERS-CoV infection. Hum Vaccin Immunother 13:1615-1624.

55. Biacchesi S, Skiadopoulos MH, Yang L, Murphy BR, Collins PL, Buchholz UJ. 2005. Rapid human metapneumovirus microneutralization assay based on green fluorescent protein expression. J Virol Methods 128:192-197.

628 **Figure Legends**

629 **FIG 1 Schematic map for establishment of MERS-CoV Nb library and generation of**
630 **NbMS10 and NbMS10-Fc Nbs.** Blood was collected from MERS-CoV RBD-Fc protein-
631 immunized alpaca post-last immunization to isolate PBMCs. RNA was then extracted to synthesize
632 cDNA via RT-PCR. This was followed by PCR amplification of the N-terminal IgG heavy-chain
633 fragment (~700 bp) including VHH gene, while the latter was used as the template to amplify the
634 VHH gene fragment (~300-450 bp). The VHH DNA sequence was further ligated into phagemid
635 vector pCANTAB5e, and transformed into *E. coli* TG1 competent cells to construct VHH library.
636 VHH phage display was carried out to isolate RBD-specific clones. After four rounds of bio-
637 panning, RBD-specific VHH coding sequence was confirmed from the selected positive clones.
638 The identified VHH coding gene containing a C-terminal His_6 or human IgG1 Fc was inserted into
639 *Pichia pastoris* yeast expression vector pPICZαA to construct NbMS10 and NbMS10-Fc,
640 respectively, for further soluble expression and purification.
641
642 **FIG 2 Characterization of MERS-CoV RBD-specific NbMS10 and NbMS10-Fc Nbs.** (A)
643 SDS-PAGE and Western blot analyses of purified NbMS10 and NbMS10-Fc. The Nbs were
644 subjected to SDS-PAGE (left) or Western blot (right), followed by detection using anti-llama
645 antibody. The molecular weight marker (kDa) is indicated on the left. (B) Detection of binding
646 between NbMS10 or NbMS10-Fc and MERS-CoV S1 (MERS-S1) or RBD (MERS-RBD) protein
647 by ELISA. The plates were coated with MERS-CoV S1-His or RBD-Fd protein (2 μg/ml),
648 followed by sequential incubation with respective Nbs, goat anti-llama, and HRP-conjugated anti-
649 goat IgG antibodies. The data are presented as mean (A450) ± SD (n = 2). Significant differences
650 (*, ** and ***) are shown in the binding of Nbs to MERS-S1 or MERS-RBD at various

concentrations. (C) The binding kinetics between NbMS10 or NbMS10-Fc and MERS-CoV RBD or S1 protein were measured by SPR. MERS-CoV RBD-Fc protein was used for binding to NbMS10 (containing a C-terminal His_6), and S1-His protein for binding to NbMS10-Fc (containing a C-terminal human Fc). (D) Detection of NbMS10 and NbMS10-Fc neutralizing activity against MERS-CoV infection (EMC2012 strain) by a micro-neutralization assay. The Nb-MERS-CoV mixtures were incubated with Vero E6 cells, and observed for the presence or absence of cytopathic effect (CPE). Neutralizing activity of Nbs was recorded as the concentration of Nbs in complete inhibition of MERS-CoV-induced CPE in at least 50% of the wells (ND_{50}). The data are expressed as mean (ND_{50}) ± standard deviation (SD) (n = 3). The experiments were repeated twice, and similar results were obtained. (-) control in (A), (B), and (D): SARS-CoV 33G4 mouse mAb.

FIG 3 Determination of mechanisms of NbMS10 and NbMS10-Fc Nbs by flow cytometry and ELISA analyses. (A-B) Flow cytometry analysis of NbMS10 and NbMS10-Fc in inhibiting the binding between MERS-CoV RBD and cell-associated hDPP4 receptor. (A) Gray shading, Huh-7 cell control. Red line, binding of MERS-CoV RBD (i.e., RBD-Fc protein, 20 μg/ml) to Huh-7 cells. Blue line, NbMS10 (a) and NbMS10-Fc (b) Nbs (10 μg/ml), or SARS-CoV 33G4 mAb control (c), inhibited RBD binding to Huh-7 cells. Percentages of inhibition (% inhibition) are shown in each graph. (B) NbMS10 and NbMS10-Fc demonstrated dose-dependent inhibition of the binding between MERS-CoV RBD and cell-associated hDPP4 in Huh-7 cells. % inhibition was calculated as RBD-Huh-7 cell binding in the presence and absence of Nbs using the following formula: (1-RBD-Huh-7-Nb/RBD-Huh-7)*100. (C) ELISA analysis of NbMS10 and NbMS10-Fc in inhibiting the binding between MERS-CoV RBD and soluble hDPP4 protein. The plates were coated with

674 MERS-CoV RBD-Fc protein (2 μg/ml), followed by sequential incubation with serial dilutions of
675 Nbs or hDPP4 protein (2 μg/ml), goat anti-hDPP4, and HRP-conjugated anti-goat IgG
676 antibodies. % inhibition was calculated as RBD-hDPP4 binding in the presence and absence of Nbs
677 using the following formula: (1-RBD-hDPP4-Nb/RBD-hDPP4)*100. Significant difference (***)
678 is shown between NbMS10 and NbMS10-Fc in inhibition of RBD-hDPP4 binding. (-) control in
679 (B)-(C): SARS-CoV 33G4 mAb. The data are presented as mean (% inhibition) ± SD (n = 2). The
680 experiments were repeated twice, and similar results were obtained.
681
682 **FIG 4 NbMS10 and NbMS10-Fc Nbs recognized conformational epitopes and mapping of**
683 **Nb's neutralizing epitope(s).** (A) Mapping of the epitope of NbMS10 by ELISA. The plates were
684 coated with RBD-Fc (RBD-WT) or respective mutant RBD proteins containing a C-terminal
685 human Fc (2 μg/ml), followed by sequential incubation with serial dilutions of NbMS10
686 (containing a C-terminal His_6), mouse anti-His and HRP-conjugated anti-mouse IgG antibodies.
687 The data are presented as mean (A450) ± SD (n = 3). (B) Inhibitory effect of NbMS10 and
688 NbMS10-Fc against infection of MERS-CoV pseudoviruses with (MERS-D539A) or without
689 (MERS-WT) D539A mutation. The data are presented as mean (% inhibition) ± SD (n = 4). (C)
690 Binding of MERS-CoV RBD with (MERS-D539A) or without (MERS-WT) D539A mutation to
691 hDPP4 protein by ELISA. The data are presented as mean (A450) ± SD (n = 4). Significant
692 difference (***) is shown between MERS-WT and MERS-D539A in binding to hDPP4. (D)
693 Detection of the binding between NbMS10 or NbMS10-Fc and MERS-CoV RBD by ELISA in the
694 presence or absence of DTT. The plates were coated with RBD-Fd protein (2 μg/ml), and treated
695 with or without DTT, followed by sequential incubation with serial dilutions of NbMS10 or
696 NbMS10-Fc, goat anti-llama and HRP-conjugated anti-goat IgG antibodies. The data are presented

as mean (A450) ± SD (n = 2). (-) control in (B) and (D): SARS-CoV 33G4 mAb. The above experiments were repeated twice, and similar results were obtained.

FIG 5 Proposed structural mechanisms for the neutralizing activity of NbMS10 and NbMS10-Fc Nbs. (A) Crystal structure of MERS-CoV RBD complexed with hDPP4 receptor (PDB ID: 4KR0). MERS-CoV RBD is colored in green, and hDPP4 is colored in cyan. RBD residue Asp539, which is critical for the binding of the Nbs to the RBD, is shown in sticks. (B) Structural role of RBD residue Asp539 at the interface between MERS-CoV RBD and hDPP4 (PDB ID: 4KR0). RBD residue Asp539 forms a critical salt bridge with DPP4 residue 267, a van der Waals interaction with RBD residue Tyr541, and a hydrogen bond with the main chain nitrogen of RBD residue Glu536. Near Asp539 is an N-linked glycan from DPP4 that forms strong and favorable van der Waals stacking with RBD residue Trp535. Dotted lines indicate hydrogen bonds, and arrows indicate van der Waals interactions. (C) Proposed structural mechanisms for the neutralizing activity of NbMS10 and NbMS10-Fc Nbs. The Nbs (colored in red) bind to the RBD epitope surrounding Asp539, disrupting the binding interactions between the RBD and DPP4 and physically blocking the binding of DPP4 to the RBD.

FIG 6 Detection of half-life of Nbs in C57BL/6 mice. Sera were collected from mice injected with NbMS10 (A), NbMS10-Fc (B), or PBS control (C) at the indicated time points, and tested by ELISA for the binding with MERS-CoV S1 protein. The plates were coated with S1-His protein (2 μg/ml), and the data are presented as mean (A450) ± SD of mice (n = 5) in each group.

719 **FIG 7 Evaluation of prophylactic and therapeutic efficacy of NbMS10-Fc in hDPP4-Tg mice.**
720 The hDPP4-Tg mice were treated with NbMS10-Fc or Trastuzumab (-) control (10 mg/kg) 3 days
721 pre-infection (A) or 1 day (B) and 3 days (C) post-infection of MERS-CoV (EMC2012 strain, $10^{5.3}$
722 median tissue culture infectious dose: $TCID_{50}$). Virus-challenged mice were monitored for 14 days
723 to evaluate survival rate (above) and body weight changes (below). The data of body weight are
724 presented as mean ± SD of mice in each group (n = 6). Significant differences (** and ***) are
725 shown between NbMS10-Fc and control groups.
726
727 **FIG 8 Conservation of residue D539 at the RBD of MERS-CoV S protein.** Schematic structure
728 of RBD and mutations of amino acid (aa) residues at the RBM of RBD among natural MERS-CoV
729 isolates. Total 482 RBM sequences (residues 484-567) derived from natural MERS-CoV isolates
730 were aligned, and residues with natural mutations are shown. Residues in the rectangle frame show
731 the RBM consensus, and the positions of corresponding residues are illustrated. The numbers on
732 the left indicate the counts of MERS-CoV isolates with the identical sequence in the analyzed
733 region.
734
735

736 **Tables**

737 **TABLE 1 Cross-neutralizing activity of MERS-CoV RBD-specific Nbs against divergent**

738 **strains of MERS-CoV**[a]

Accession No.	Isolate year	Host	Region	RBD mutation(s)[b]	ND_{50} (μg/ml)[c]	
					NbMS10	NbMS10-Fc
AFS88936	2012	Human	Saudi Arabia	—	0.046	0.047
AGV08379	2012	Human	Saudi Arabia	D509G	0.067	0.067
AGV08584	2012	Human	Saudi Arabia	V534A	0.979	0.026
AHI48528	2013	Human	Saudi Arabia	A431P, A482V	0.121	0.005
AHI48733	2013	Human	Saudi Arabia	A434V	0.049	0.003
AHC74088	2013	Human	Qatar	S460F	0.031	0.005
AHY22545	2013	Camel	Saudi Arabia	K400N	0.088	0.014
AHY22555	2013	Camel	Saudi Arabia	A520S	0.040	0.044
AID55090	2014	Human	Saudi Arabia	T424I	0.044	0.005
AID55087	2014	Human	Saudi Arabia	Q522H	0.156	0.005
ALB08322	2015	Human	South Korea	D510G	0.003	0.005
ALB08289	2015	Human	South Korea	I529T	0.004	0.011

739

740 [a]A pseudovirus-based neutralization assay was performed to evaluate the cross-neutralizing activity
741 of Nbs against divergent MERS-CoV isolates. Pseudotyped MERS-CoV mutants were generated
742 containing the corresponding mutations in the RBD of S protein of MERS-CoV representative
743 isolates from years 2012–2015. [b]RBD residues mutated in the S protein of the respective
744 pseudotyped MERS-CoV mutants are indicated. The pseudotyped MERS-CoV expressing S
745 protein of the EMC2012 strain (Accession number: AFS88936) was considered to be the prototype
746 pseudovirus. [c]ND_{50} was determined as 50% neutralization dose using a pseudotyped MERS-CoV
747 neutralization assay.

748
749
750
751

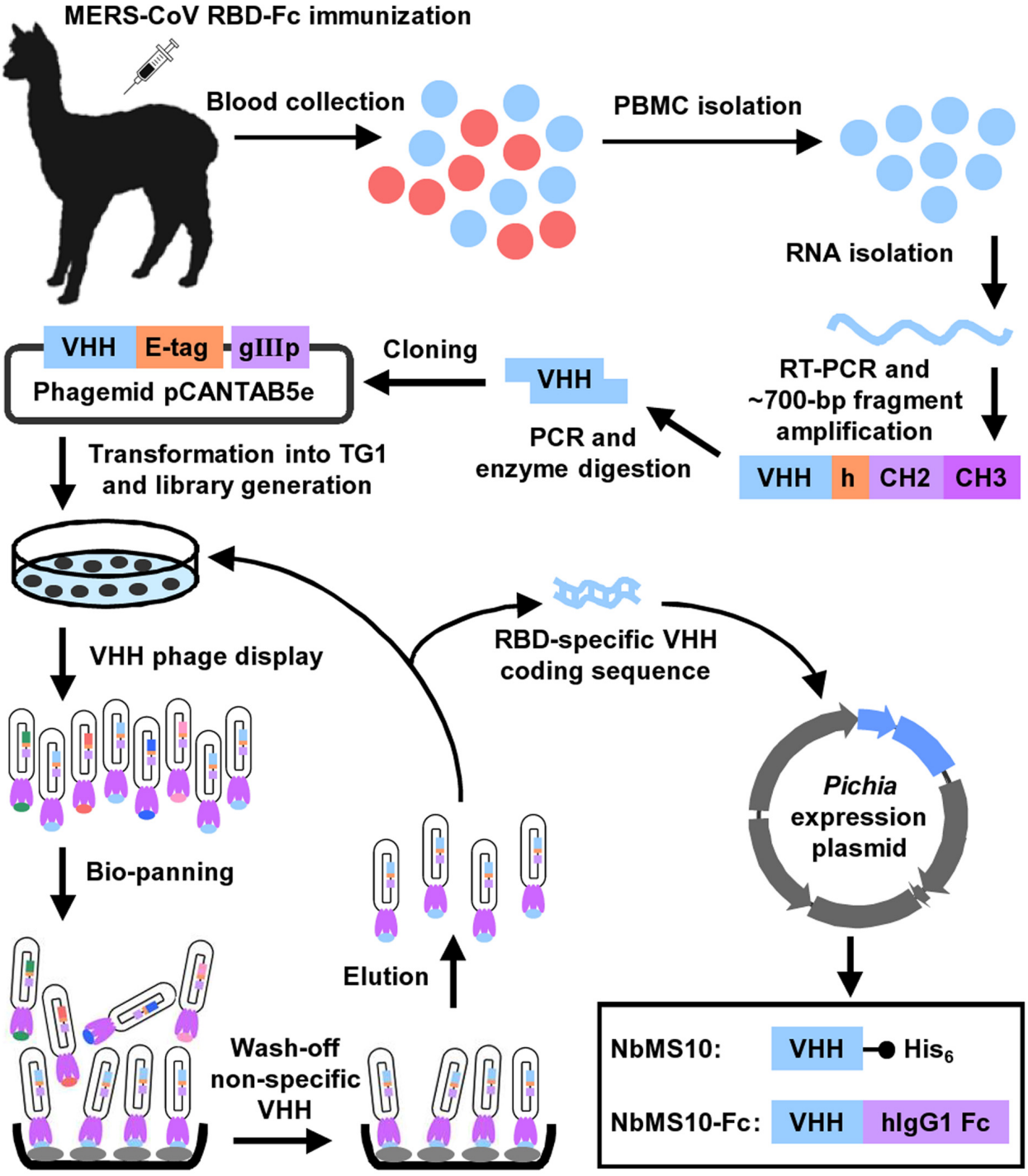

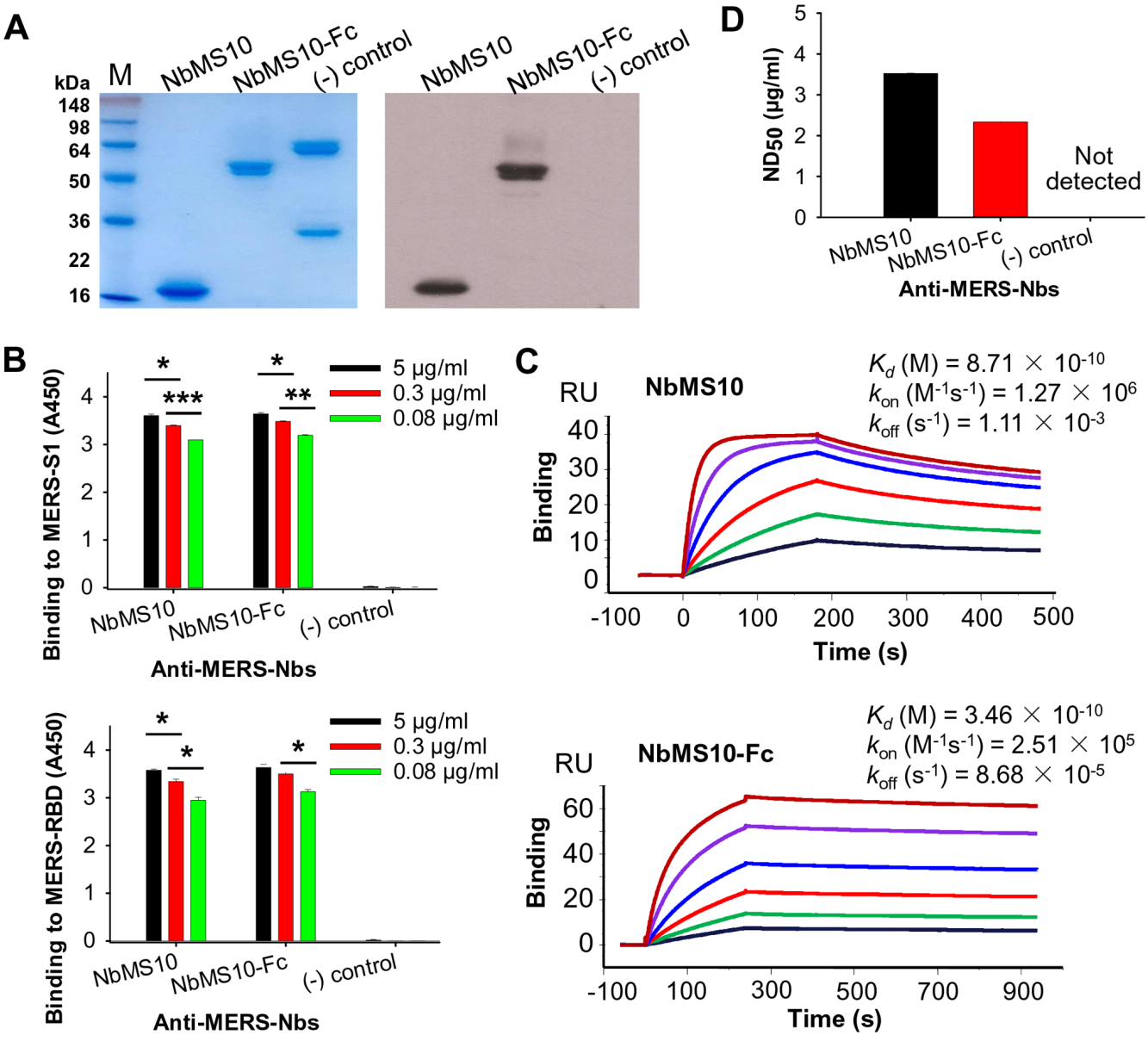

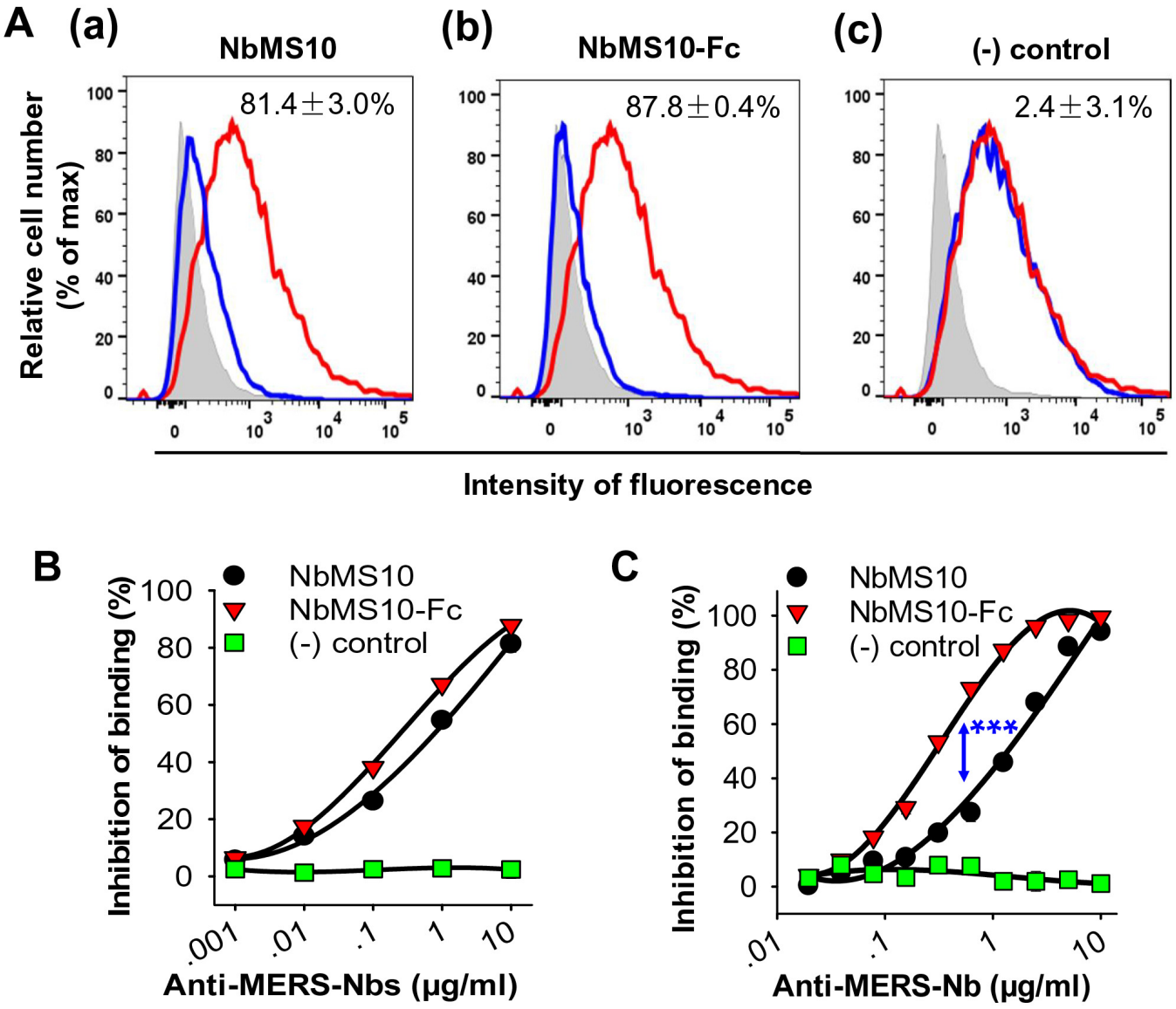

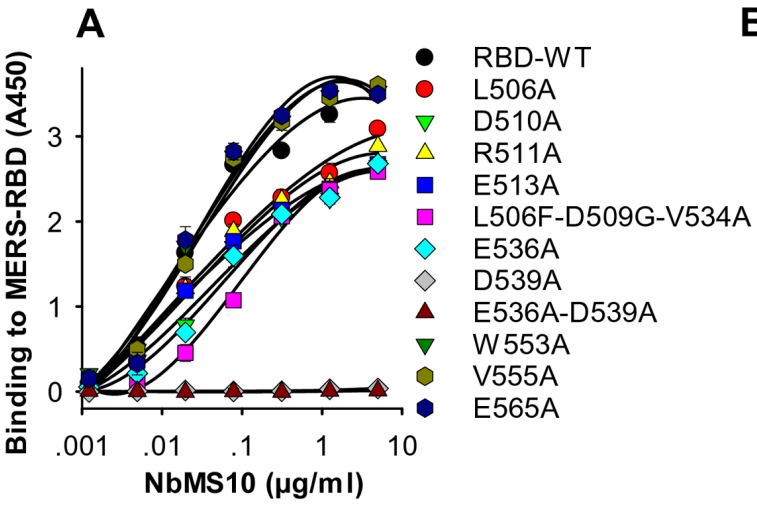

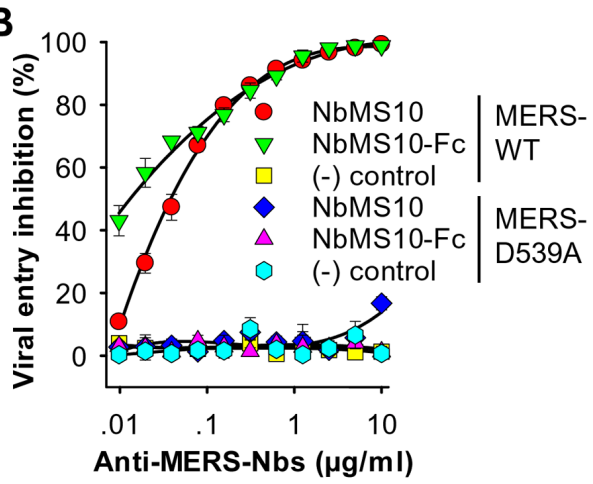

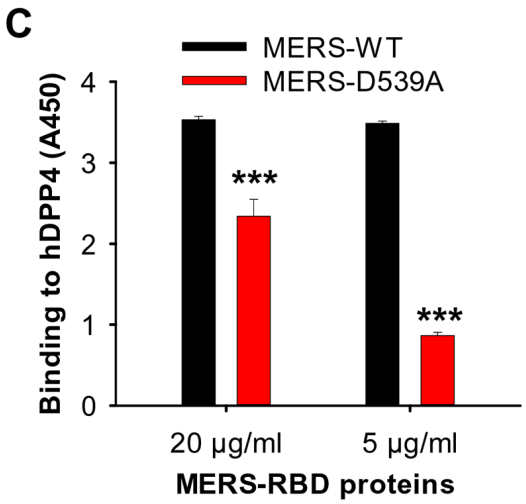

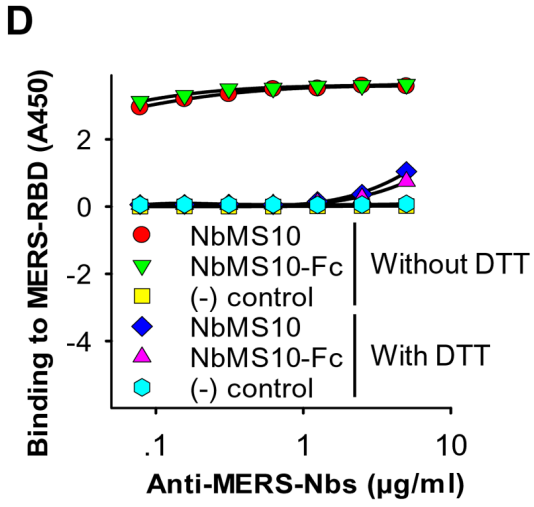

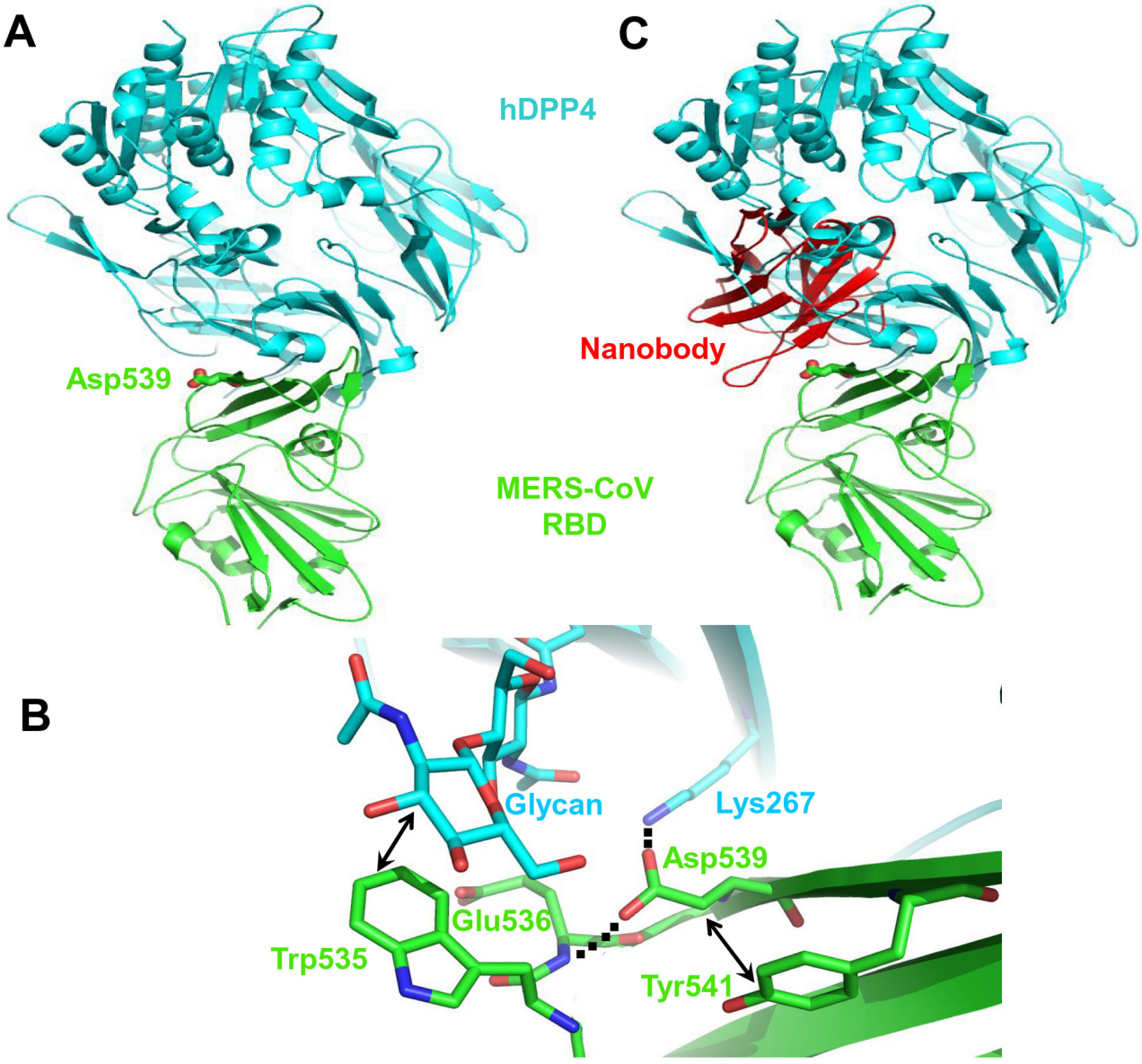

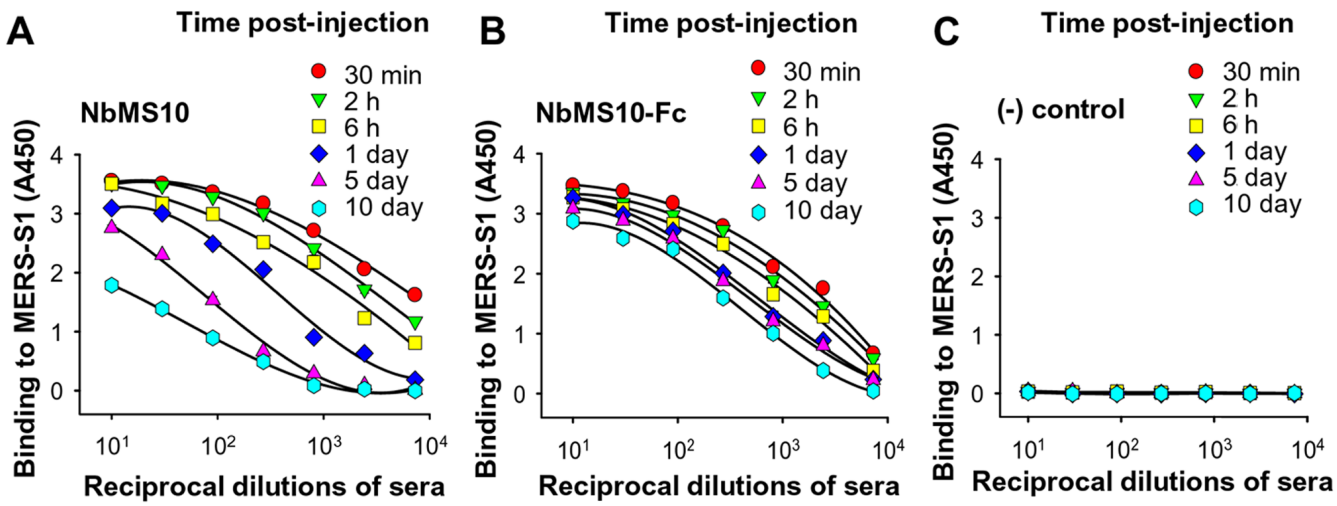

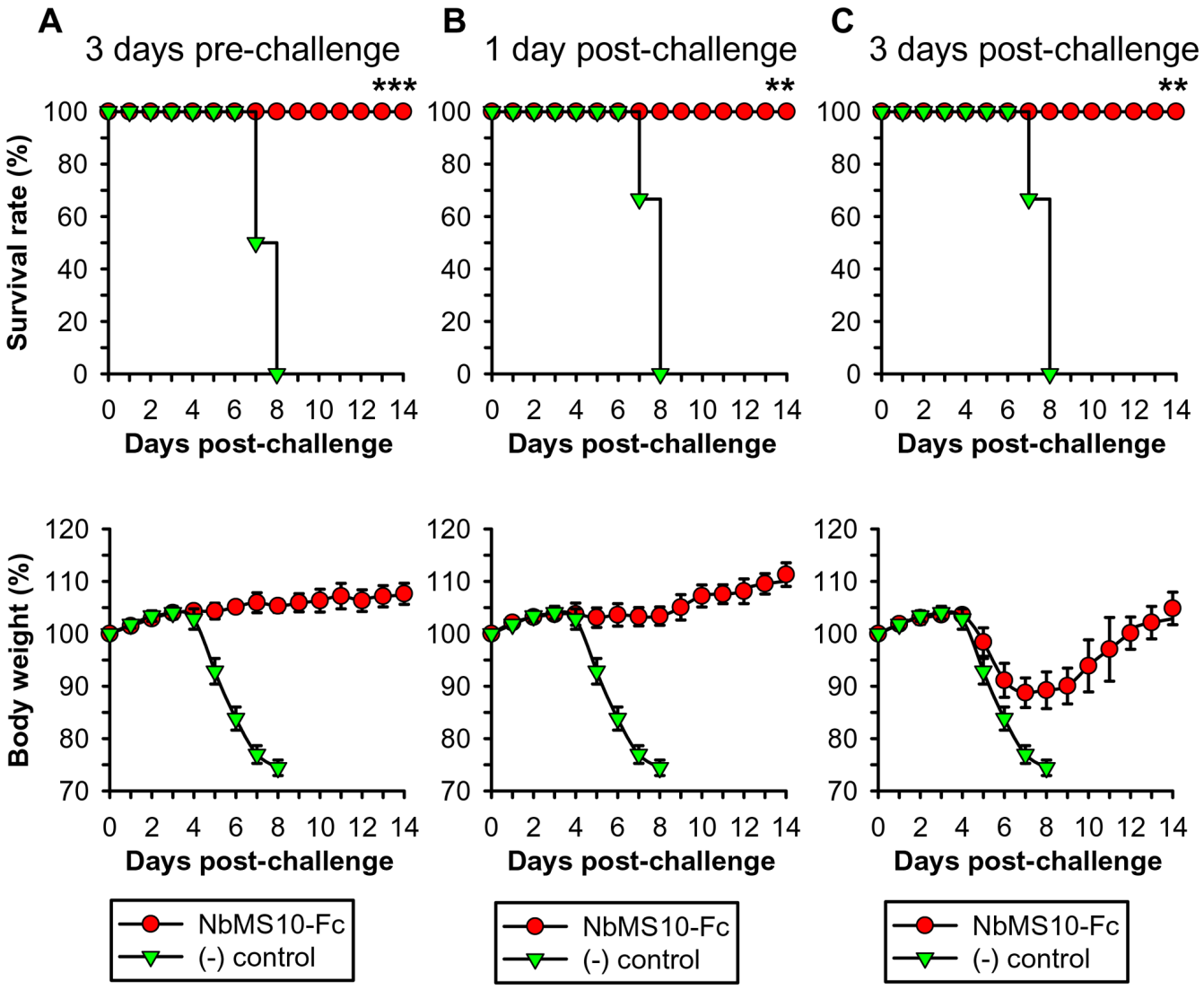

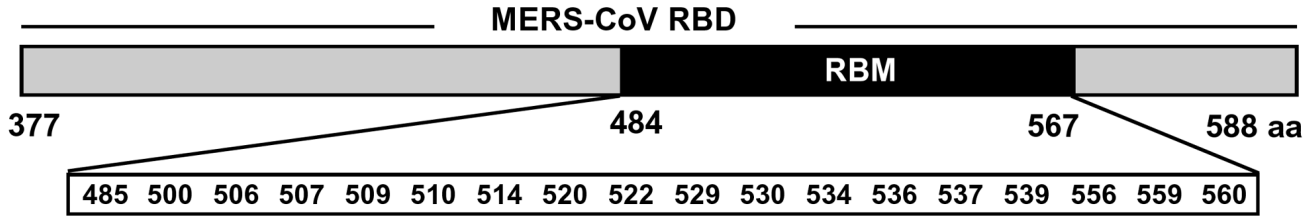

	485	500	506	507	509	510	514	520	522	529	530	534	536	537	539	556	559	560
(418)	P	I	L	L	D	D	V	A	Q	I	V	V	E	D	D	A	S	T
(26)	-	-	-	-	-	-	-	-	-	T	-	-	-	-	-	-	-	-
(7)	-	-	-	-	-	G	-	-	-	-	-	-	-	-	-	-	-	-
(4)	-	-	-	-	-	-	-	-	-	-	-	-	-	-	-	-	-	I
(3)	-	-	-	-	G	-	-	-	-	-	-	-	-	-	-	-	-	-
(2)	S	-	-	-	-	-	-	-	-	-	-	-	-	-	-	-	-	-
(2)	-	-	F	-	-	-	-	-	-	-	-	-	-	-	-	-	-	-
(2)	-	-	-	P	-	-	-	-	-	-	-	-	-	-	-	-	-	-
(2)	-	-	-	-	-	-	-	-	-	-	-	A	-	-	-	-	-	-
(2)	-	-	-	-	-	-	-	-	-	-	-	-	K	-	-	-	-	-
(2)	-	-	-	-	-	-	-	-	-	-	-	-	-	-	-	V	-	-
(2)	-	-	-	-	-	-	L	-	-	-	-	-	-	-	-	-	-	-
(1)	-	F	-	-	-	-	-	-	-	-	-	-	-	-	-	-	-	-
(1)	-	-	-	-	-	-	-	-	-	-	-	-	-	-	-	-	P	-
(1)	-	-	-	-	H	-	-	-	-	-	-	-	-	-	-	-	-	-
(1)	-	-	-	R	-	-	-	-	-	-	-	-	-	-	-	-	-	-
(1)	-	-	-	-	-	-	-	S	-	-	-	-	-	-	-	-	-	-
(1)	-	-	-	-	-	-	-	-	H	-	-	-	-	-	-	-	-	-
(1)	-	-	-	-	-	-	-	-	-	-	L	-	-	-	-	-	-	-
(1)	-	-	-	-	-	-	-	-	-	-	-	L	-	-	-	-	-	-
(1)	-	-	-	-	-	-	-	-	-	-	-	-	-	E	-	-	-	-
(1)	-	-	-	-	-	-	-	-	-	-	-	-	-	-	N	-	-	-